Cellulose (2014) 21:1619–1629
DOI 10.1007/s10570-014-0238-y

ORIGINAL PAPER

Nanopaper from almond (*Prunus dulcis*) shell

Iñaki Urruzola · Eduardo Robles · Luis Serrano · Jalel Labidi

Received: 7 October 2013 / Accepted: 11 March 2014 / Published online: 20 March 2014

Abstract Five pulping methods using different reagents were used for the delignification of almond shells: sodium hydroxide 7.5 % v/v for 24 h at 60 °C, potassium hydroxide 7.5 % v/v for 24 h at 60 °C, formic acid/water 90/10 v/v, organosolv with ethanol/water 60/40 v/v and sodium hydroxide 15 % v/v in an autoclave for 90 min at 120 °C. The resulting cellulose pulps were evaluated using TAPPI standard methods and X-ray diffraction (XRD) to determine the lignin content and crystallinity changes. After pulping, fibers were bleached with sodium chlorite and hydrogen peroxide to obtain pure cellulose. The resulting pulps were characterized by XRD and thermogravimetry to determine the cellulose purification rates and changes in crystallinity. Then, the different pulps were acetylated, hydrolyzed and homogenized to obtain cellulose nanofibers. Nanofiber sizes were assessed by atomic force microscopy and XRD to evaluate the effect of hydrolysis on nanofibers. Finally, nanopaper sheets were produced and the properties were compared to conventional micropaper. The different treatments influenced the amount of lignin eliminated, which had a direct relationship on the subsequent bleaching treatments to obtain pure cellulose. Hence, the different chemical methods influenced the crystallinity of the fibers which also influenced the yield of cellulose nanofibers and different nanopapers.

Keywords Almond shell · Cellulose · Lignin · Nanofibers · Nanopaper

I. Urruzola · E. Robles · L. Serrano · J. Labidi (✉)
Chemical and Environmental Engineering Department, University of the Basque Country, Plaza Europa, 1, 20018 Donostia-San Sebastián, Spain
e-mail: jalel.labidi@ehu.es

Introduction

In recent years, the use of cellulose nanofibers has been increasing. Currently, about 100 million tons of cellulose are produced annually in plants around the world (Delmer and Amor 1995; Annergren 1996), but obtaining them from agroforestry raw materials like flax, eucalyptus, sisal, etc. represents a challenge as non-cellulosic components are present in the structure of these materials.

Cellulose is one of the most important biopolymers found in nature due to its biocompatibility, biodegradability and low cost. Cellulose is a polysaccharide composed exclusively of glucose molecules. It is rigid, insoluble in water and contains from several hundred to several thousand units of β-glucose. Cellulose is the most abundant organic biomolecule as it forms the bulk of terrestrial biomass (Fratzl 2003; Vincent 1999; Bidlack et al. 1992). Cellulose has different applications in industry; among them, the most important is the production of pulp and paper using different types of raw materials and processes.

Annually, around 2.31 million tons of almonds (with shells) are produced, of which 0.8–1.7 million tons corresponds to almond shells (Pirayesh and Khazaeian 2012). The shell of the common almond (*Prunus dulcis*) presents a high content of crystalline cellulose, but also a considerable amount of lignin. This residue can be used as a source of cellulose nanofibers or lignin bio-products.

Chemical and mechanical treatments or combinations of both are used for the production of cellulose nanofibers (Jonoobi et al. 2009). The isolation of cellulose nanofibers from lignocellulosic feedstock requires, as a first step, the removal of lignin using chemical treatments (Serrano et al. 2011). Industrially, bleached cellulose pulp is obtained using two process stages: pulping and bleaching. The objective of pulping is to remove the lignin and to release cellulose fibers, thereby separating cellulose from the other components. This process can be either mechanical or chemical. The most widely used pulping process in the world is the Kraft process. Moreover, bleaching is performed as a chemical treatment in stages and under different operating conditions. The main chemical reagents used are elemental chlorine (Cl_2), chlorine dioxide (ClO_2) and hydrogen peroxide (H_2O_2).

Mechanical treatments such as high pressure homogenization and ultrasound techniques are used to reduce the size of the cellulose fibers to the nano-size scale where the properties of the cells vary considerably (Lee et al. 2009; Chen et al. 2011a).

The output of this pulp to different applications is an important aspect of the paper industry within the so-called biorefinery concept. Nanopaper production is essentially similar to the process used to produce regular (micro) paper; nanofibers are placed in suspension to prepare a packed gel by filtering a previously prepared water suspension. As water evaporates, capillary forces provide attraction between individual nanofibers (Sehaqui et al. 2010), thus forming the base of the nanopaper. Several methods to make the final form are being studied. Nanopaper structures show an interesting combination of elastic modulus, tensile strength and toughness (Henriksson et al. 2008), thus making this an alternative material for multiple applications, depending on the requirements of final use.

In this study, nanopaper production was carried out by hot pressing of almond shell nanofibers. The mechanical properties of the nanopapers were compared to those of regular micropaper. A range of methods was assessed to remove lignin from the lignocellulosic materials. To select the most appropriate process, several factors must be considered, as the effect of an acid or basic basis, is different on the cellulose microfibrils. For example, acid treatments are known to eliminate the complete amorphous part of a fiber, thereby increasing the crystallinity but reducing the length of the fibers (Chen et al. 2011b; Wang et al. 2007).

Experimental section

Materials

Almond shells were supplied by a local farmer and originated from almond trees (*P. dulcis*) cultivated in la Rioja (Spain) belonging to the varieties called Marcona and Largueta. The composition of the raw material was as follows: extracts 0.72 ± 0.02, moisture 10.76 ± 0.06, lignin 52.59 ± 0.14, hemicelluloses 8.57 ± 0.06 and α-cellulose 41.28 ± 0.36, which was obtained according to standards methods (Tappi 2007) and procedures in the literature (Rowell 1983).

Chemical elimination of the non-cellulosic content

Different chemical treatments and combinations were used (Fig. 1). Before carrying out the treatments, pretreatment was performed for the elimination of residual extracts. Almond shells were pretreated for 24 h in an alkaline sodium hydroxide (1 %) solution. After that, five different methods of pulping were used (Table 1) to obtain cellulose pulp. For this purpose, 250 g of almond shells were used for each treatment. In the first process, the raw material was treated with sodium hydroxide 7.5 % v/v solution for 24 h at 60 °C (Urruzola et al. 2013a); while in the second process, a potassium hydroxide solution (7.5 % v/v) was used for 24 h at 60 °C (Zuluaga et al. 2009). In the third process, a solution of formic acid/water 90/10 v/v was used for 90 min at 130 °C (Dapía et al. 2002). In the fourth process, the raw material was treated with an organosolv process using ethanol/water 60/40 v/v for 90 min at 130 °C (Ni and Van Heiningen 1996). In the fifth process, the material was submitted to sodium hydroxide (15 % v/v) in an autoclave for 90 min at

Fig. 1 Scheme of the nanofiber extraction process

Table 1 Chemical treatments used and their conditions

	Reaction	Temperature (°C)	Time (h)
T1	Sodium hydroxide 7.5 % v/v	60	24
T2	Potassium hydroxide 7.5 % v/v	60	24
T3	Formic acid/water 90/10 v/v	130	1.5
T4	Ethanol/water 60/40 v/v	130	1.5
T5	Sodium hydroxide 15 % v/v	120	1.5

120 °C (Arni et al. 2007). After each treatment, the obtained pulp was washed and dried.

The obtained pulps were submitted to a sequence of bleaching treatments performed by two sodium chlorite treatments and one peroxide hydroxide treatment. Sodium chlorite bleaching treatments were performed by adding a 23 % solution of sodium chlorite (25 % w/w) in 0.1 L of water per gram of pulp for 2 h at 75 °C in a water bath (Escarnota et al. 2011; Sun et al. 2000, 2002). On the other hand, the hydroxide peroxide bleaching treatments were performed using 1 g of sodium chlorite, 2 g of hydroxide peroxide, 0.5 g of pentetic acid (DTPA) and 2 g of $MgSO_4$ in a water bath for 150 min at 70 °C.

Mechanical extraction of cellulose microfibrils

Before mechanical treatment, acetylation was carried out to destroy the microstructure. For this purpose, 0.6 g of each bleached pulp were added to a solution containing 2 mL of nitric acid and 12 mL of acetic acid and heated to the boiling point for 30 min with continuous stirring. Then, the obtained fibers were washed and dried. After acetylation, a hydrolysis process was carried out, using 1 g of acetylated pulp in a solution containing 8.75 mL of H_2SO_4 and heated to 45 °C for 1 h (Urruzola et al. 2013a). Then, the fibers were washed and dried. This treatment was used to increase the crystallinity of pulps and thus improve the mechanical properties.

One gram of each hydrolyzed pulp was dispersed in 250 mL of water. The suspension was treated in an ultrasonic bath for 3 h to separate the fibril bundles. Homogenization of the cellulose fibrils was performed in a Niro Soavi homogenizer using 30 passes at a pressure of 1,000 bar. The fundamental mechanism of the high-pressure homogenizer is to pump a fluid stream against itself within interaction chambers of fixed geometry at very high energy, directly resulting in the breakup and dispersion of the slurry. High pressure, high velocity and a variety of forces on the fluid stream are capable of generating shear rates within the product stream, reducing particles to the nanoscale (Urruzola et al. 2013b).

Fabrication of nanopapers

Homogenized solutions were vacuum filtered through a 0.45 μm nylon filter to obtain a homogeneous gel. This gel was then dried in an oven for 5 min at 105 °C to remove excess humidity and then submitted to a series of pressing cycles and press curing. For this purpose, the previously dried gel was placed between two copper plates in a Santec hydropneumatic molding press (30 tons), and four cycles of increasing pressure were performed at a constant temperature to avoid shape malformations in the paper due to high pressure. The cycles were performed at 10, 20, and 40 bar at 100 °C. Finally, a curing pressure of 200 bar at 100 °C was carried out for 25 min.

Atomic force microscopy (AFM)

AFM images were obtained operating in tapping mode with a scanning probe microscope (Nanoscope IIIa, Multimode™ from Digital Instruments, Veeco) equipped with an integrated silicon tip cantilever with a resonance frequency of 300 kHz. To obtain representative results, different regions of the samples were scanned. Similar images were obtained, thus demonstrating the reproducibility of the results.

X-ray diffraction (XRD)

The X-ray powder diffraction patterns were collected by using a PHILIPS X'PERT PRO automatic diffractometer operating at 40 kV and 40 mA, in theta–theta

configuration, using a secondary monochromator with Cu-Kα radiation (λ = 1.5,418 Å) and a PIXcel solid state detector (active length in 2θ 3.347°). The powdered samples were mounted on a zero background silicon wafer fixed in a generic sample holder. Data were collected from 5 to 70° 2θ (step size = 0.026 and time per step = 80 s) at RT. A fixed divergence and antiscattering slit was used to provide a constant volume of sample illumination.

There are plenty methods to analyze crystalline structures (French and Cintrón 2013; French 2014) in this study, the crystallinity index (CI) was calculated from the heights of the 2 0 0 peak (I_{200}, 2θ = 22.6°) and the intensity minimum between the 2 0 0 and 1 1 0 peaks (I_{am}, 2θ = 18°) using the Segal method (Chen et al. 2011a).

$$\mathrm{CI}\,(\%) = \left(1 - \frac{I_{am}}{I_{200}}\right) \times 100$$

I200 represents both crystalline and amorphous material, whereas I_{am} represents the amorphous material.

Fourier transform infrared spectroscopy (FT-IR)

The FTIR spectra were recorded on a Perkin-Elmer 16 PC instrument, by direct transmittance with an MKII Golden Gate SPEACAC accessory in the range of 800–4,000 cm^{-1} with a resolution of 8 cm^{-1} and 20 scans.

Thermogravimetric analysis (TGA)

The thermal stability of each sample was determined using a thermogravimetric analyzer (Pyris 6 Perkin Elmer) with a heating rate of 10 °C min^{-1} in a nitrogen atmosphere.

Density and porosity measurements

The density of the nanopapers was determined by measuring their weight and dividing this value by its volume. The volume was calculated from the thickness of the nanopapers (determined by a digital caliper) and its area. Porosity was estimated from the density of the nanopaper by taking 1,460 kg m^{-3} as the density of cellulose (Sun 2008) using the following equation:

$$Porosity = 1 - \rho_{nanopaper}/\rho_{cellulose}$$

The mechanical properties of porous materials depend directly on the relative density $\rho_{\mathrm{nanopaper}}/\rho_{\mathrm{cellulose}}$ (Gibson and Ashby 1997) and therefore on the porosity. The real porosity values may be slightly lower than the present estimates since the real $\rho_{\mathrm{cellulose}}$ can be lower than 1,460 kg m^{-3}.

Mechanical properties

Tensile tests of the nanopapers were performed using MTS Insight 10 equipment provided with pneumatic clamps (Advantage Pneumatic Grips) and with a 250 N loading cell and a speed of 5 mm min^{-1}. Samples were prepared, dogbone-shaped, 38 mm long, with a width of 5 mm and at a thickness of 0.07–0.09 mm. The starting distance between the clamps was 20 mm. The values quoted are the average of eight measurements.

Results and discussion

Extraction of pure cellulose

After different chemical treatments for the elimination of almond shell lignin, several characterizations were carried out to analyze the amount of lignin removed with each treatment. The resulting pulps were characterized with TAPPI standard methods and the values are shown in Table 2.

The lignin content was significantly reduced after all treatments. Using the organosolv process, the lignin content decreased by 10 %; this decline was lower than that obtained with other treatments, but a higher purity lignin can be obtained. The other treatments resulted in more delignification, but the

Table 2 Chemical composition of almond shell before and after chemical treatments

Analysis (%)	Extract	Moisture	Lignin
Almond shell	0.72 ± 0.02	10.76 ± 0.06	52.59 ± 0.14
Organosolv	5.28 ± 0.02	30.55 ± 0.06	43.21 ± 0.06
NaOH 15 %	3.28 ± 0.02	19.03 ± 0.06	42.76 ± 0.06
KOH	1.06 ± 0.02	0.435 ± 0.06	39.92 ± 0.06
NaOH 7.5 %	1.35 ± 0.02	0.432 ± 0.06	35.34 ± 0.06
Formic acid	4.21 ± 0.02	2.16 ± 0.06	30.72 ± 0.06

Fig. 2 Pulps after chemical treatment. **a** Organosolv, **b** NaOH 15 %, **c** KOH, **d** NaOH 7.5 %, **e** formic acid

most effective chemical treatment in order to remove lignin was formic acid with a 30 % reduction.

Figure 2 shows the different pulps obtained after chemical treatments, where it can be seen how the pulp color became lighter as the lignin content decreased, except in the case of formic acid. This treatment imparts dark color to the pulp even though this method is the most effective in reducing the lignin content.

After the first chemical treatment, the pulps were submitted to a sequence of bleaching treatments to eliminate the residual lignin. Figure 3 shows a comparison of the FT-IR spectra of different pulps before the bleaching treatments. The signals at 3,345, 2,920 and 2,860 cm^{-1} are characteristic of stretching vibrations of OH and CH groups, respectively. The signal at 2,920 cm^{-1} corresponds to CH_3 groups and the signal at 2,860 cm^{-1} corresponds to CH_2 groups. The peak at 1,645 cm^{-1} can be attributed to the bending mode of the absorbed water in carbohydrates. The band at 1,420 cm^{-1} corresponds to CH_2 bending and the one at 1,215 cm^{-1} originates from the OH in plane-bending cellulose (Sun et al. 2004a, b). The adsorption band at 1,150 cm^{-1} can be attributed to C–O anti-symmetric bridge stretching. Finally, the peak at 890 cm^{-1} is characteristic of β-glycosidic linkages between glucose units (Buschle-Diller et al. 2005).

Figure 4 shows the TGA of the five different samples, where it can be observed that the

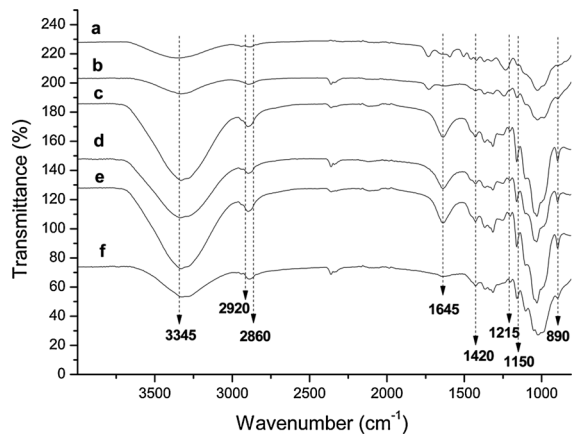

Fig. 3 FT-IR spectra of the **a** almond shell, **b** organosolv, **c** NaOH 15 %, **d** KOH, **e** NaOH 7.5 %, **f** formic acid

thermograms correspond to pure cellulose, demonstrating that the treatments were successful.

Due to the reduced decomposition temperature of hemicellulose, lignin and pectin (Moran et al. 2008), the curve of the original almond shell showed an early weight loss around 210 °C, which reached a dominant peak at 350 °C on the DTG curve, i.e. the pyrolysis temperature of cellulose. On the other hand, the chemically-purified cellulose fibers showed a higher decomposition temperature at 350 °C. The higher

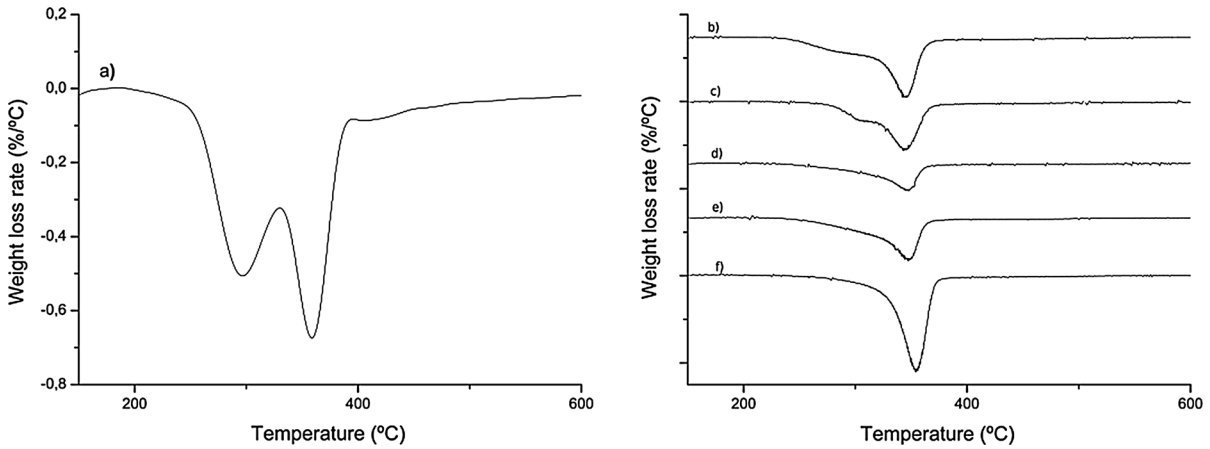

Fig. 4 DTG spectra of **a** almond shell, **b** organosolv, **c** NaOH 15 %, **d** KOH, **e** NaOH 7.5 %, **f** formic acid

temperature of thermal decomposition of the purified cellulose fibers is related to the partial removal of hemicellulose and lignin from the fibers (Alemdar and Sain 2008).

Nanofiber yield

The size of pulp fibers is in the range of several microns. Therefore, a series of chemical and mechanical treatments was carried out in order to reduce the fiber dimensions to the nanoscale. After chemical treatments involving acetylation and hydrolysis, the fiber size was considerably reduced to a few microns. However, to obtain pure nanofibers, it was still necessary to perform a mechanical treatment, which in this case was high pressure homogenization. After this treatment, the expected fiber size was achieved. Figure 5 shows AFM images of the nanofibers in each treatment obtained after high pressure homogenization.

The nanofibers had a specific shape and size depending on the treatment they were subjected to. Nanofibers treated with formic acid were short, i.e. between 0.1 and 0.5 μm in length to a maximum of 0.9 μm. With respect to the diameter, 70 % of the fibers had a width of 50–60 nm. This type of nanofiber, which is short and thin, has these dimensions due to the acid treatment used in the pulping stage. The fibers resulting from acid treatments are usually shorter in length because amorphous components are removed as the amorphous part of cellulose (Charreau et al. 2013).

In the case of nanofibers treated with organosolv, NaOH 7.5 % and NaOH 15 %, the average length was close to 1 μm. Of the nanofibers treated with organosolv, some fibers were up to 1.5 μm long and of the nanofibers treated with NaOH 7.5 %, some fibers were up to 3 μm long. However, the diameter of these three types of nanofibers differed significantly as nearly 80 % of the fibers treated with NaOH 15 %were in the range of 0.8–1 μm wide and 60 % of fibers treated with organosolv were in the range of 0.6–0.8 μm wide. The fibers treated with NaOH 7.5 % were thinner, with 70 % of the nanofibers with a diameter between 0.4 and 0.5 μm.

Finally, the nanofibers treated with KOH were the largest and thinnest fibers. The average length of these nanofibers ranged from 1.5 to 2 μm, but some fibers were up to 5 μm long. The diameter of these nanofibers was 0.4–0.6 μm for nearly 100 % of the fibers.

X-ray diffraction

The almond shell, due to its natural function of protecting the seed, is a hard raw material with high crystallinity. XRD measurements showed that almond shell had 59.17 % crystallinity, which compared with ramie that has 74 % and cotton that has crystallinities over 80 %, can be considered as a competitive crystalline cellulose (Yuan et al. 2013; Maiti et al. 2013).

After pulping treatments (Table 3), the crystallinity of the samples increased slightly; KOH was the most

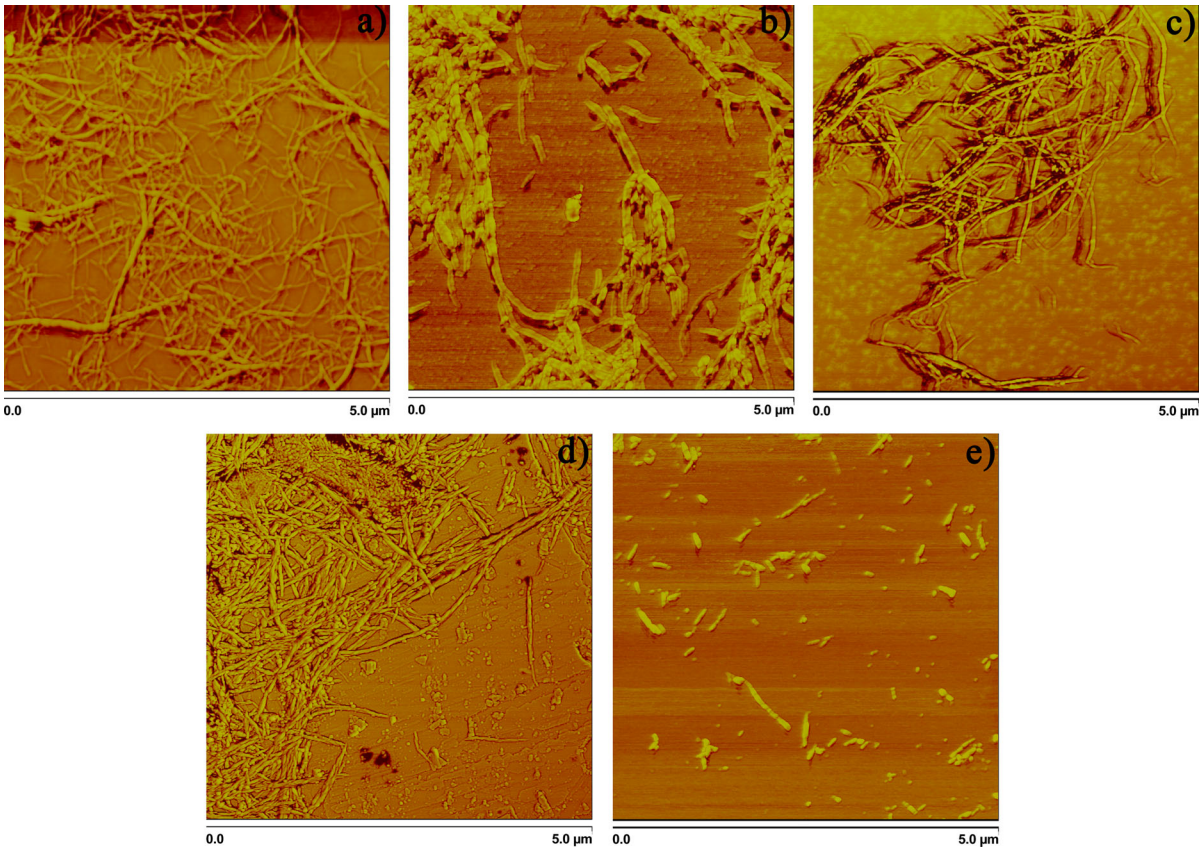

Fig. 5 AFM images of the pulps. **a** organosolv, **b** NaOH 15 %, **c** KOH, **d** NaOH 7.5 %, **e** formic acid

successful reagent of the basic treatments increasing the crystallinity to 72.68 %. Moreover, acid treatment affected the amorphous region of cellulose, increasing the crystallinity value by 3 % (Alemdar and Sain 2008; Charreau et al. 2013; Li et al. 2009). When these fibers were treated by acetylation and hydrolysis, the amorphous region of pure cellulose was affected by the acids, and the crystallinity of all the samples increased, obtaining values of about 80 % for each sample. After homogenization, the crystallinity was not analyzed because the nanofibers obtained after mechanical treatment did not show significant differences in crystallinity compared to non-homogenized fibers (Lee et al. 2009; Chen et al. 2011a). This high crystallinity is an aspect to consider as it may enhance the mechanical properties of the nanopapers.

The spectra of the KOH treated fibers are presented in the XRD results (Fig. 6), showing peaks around $2\theta = 16^\circ$ and 22.6°. The results of crystallinity suggest that the cellulose crystalline structure changed during different chemical treatments.

Table 3 Crystallinity of samples after chemical treatment

	Pulping (%)	Hydrolyzed + homogenized (%)
Formic acid	75.73	80.57
NaOH 15 %	69.35	76.95
Organosolv	62.51	78.23
NaOH 7.5 %	69.13	79.79
KOH	72.68	78.69

Mechanical properties

Stress–strain curves and mechanical properties obtained from uniaxial tensile tests are presented in Fig. 7 and Table 4. It can be observed in the KOH

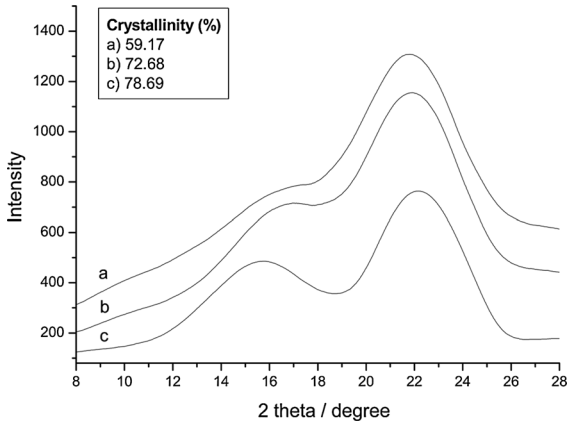

Fig. 6 X-ray diffraction results: **a** almond shell, **b** after KOH pulping, **c** after KOH pulping, acetylation and hydrolysis treatment

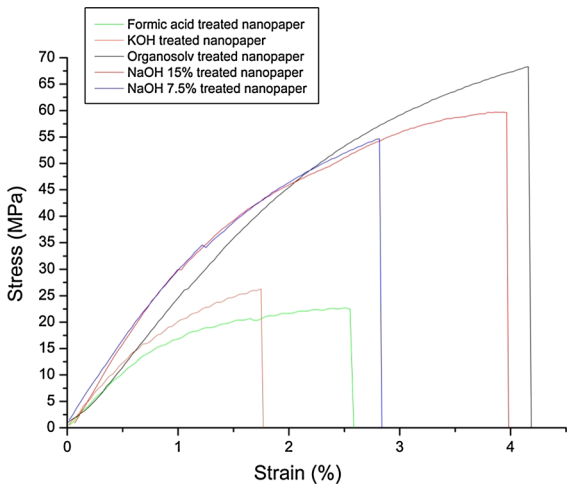

Fig. 7 Tensile stress–strain curves for different nanopapers

treated cellulose nanofibers that the modulus and ultimate tensile strength were 4,300 and 26.02 MPa, respectively. The porosity of the different cellulose nanopapers did not vary significantly; therefore, most of the nanopapers presented a porosity of about 22 % with no relevant variations, with the exception of KOH cellulose nanofibers obtained from almond shells in which the porosity reached up to 28 %. This phenomenon was due to the intrinsic relationship between porosity and mechanical properties as they are inversely proportionally related.

The low porosity of the other samples is associated with the close-packing properties of materials with high crystallinity; considering that the crystallinity of cellulose nanofibers from almond shells was around 80 %, the small amount of space between fibers prevents pore formation, thus imparting better mechanical properties. Nanopaper from organosolv treated cellulose nanofibers had a modulus of 5,300 MPa and a tensile strength of 65.14 MPa, which is remarkably close to the modulus and tensile strength of NaOH 7.5 % treated nanofibers at 5,600 and 62.70 MPa, respectively. On the other hand, the nanopaper obtained with NaOH 15 % treatment resulted in slightly lower values with respect to the previous two methods, resulting in a modulus of 4,900 MPa and a tensile strength of 56.17 MPa; notwithstanding, the porosity was similar with these three methods. This may be related to the morphology of the nanofibers as explained previously in the AFM results where nanofibers treated with NaOH 15 % had lower dimensions. Due to this, relatively poor mechanical properties were expected for the paper crafted using this method.

Finally, the nanopaper made from formic acid treated nanofibers was composed mainly of short and thin fibers as explained above, which had corresponding effects on its mechanical properties. Although the porosity in the case of formic acid treated nanofibers was lower than those of organosolv and NaOH 7.5 % treated nanofibers, the mechanical properties did not present an improvement with respect to the other two methods as expected. This may be due to the

Table 4 Porosity and mechanical properties of nanopapers

	Load (N)	Tensile stress (MPa)	Strain (%)	Modulus (GPa)	Porosity (%)
Organosolv	24.00 ± 1.27	65.14 ± 3.03	4.19 ± 0.19	5.31 ± 346.14	23
NaOH 7.5 %	24.21 ± 2.53	62.70 ± 7.04	2.85 ± 0.24	5.62 ± 170.00	23
NaOH 15 %	22.13 ± 2.57	56.17 ± 6.30	3.86 ± 0.04	4.97 ± 495.93	22
KOH	10.67 ± 0.25	26.02 ± 1.80	1.74 ± 0.14	4.36 ± 318.38	28
Formic acid	11.63 ± 0.77	22.94 ± 1.92	2.51 ± 0.10	3.80 ± 478.49	20

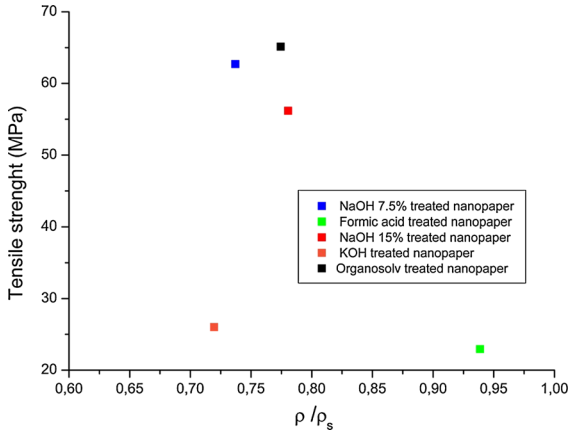

Fig. 8 Young's modulus as a function of relative density ρ/ρ_s

morphology of the fibers, which were not suitable for paper manufacturing as this paper had a modulus of 3,800 MPa and a tensile strength of 22.94 MPa.

Mechanical properties from almond shell nanopaper are not as good as others reported previously, this could be due to the aspect ratio of the obtained nanofibers that is between 1 and 10 depending on the selected delignification method; aspect ratio previously reported were above 25 (Pelissari et al. 2014). This can be assumed as an evidence of the influence that the aspect ratio has in the performance of the nanopaper when submitted to tensile tests (Iwamoto et al. 2014).

Figure 6 shows the comparison between the stress–strain curves of all nanopapers made with the different chemical treatments. Organosolv, NaOH 7.5 % and NaOH 15 % treated nanopapers had much greater tensile strength and larger strain to failure than the others. Differences in the shapes of the stress–strain curves occurred due to the particular characteristics in the deformation of the nanofibers and the interaction between the nanofibers in each kind of nanopaper.

Table 4 contains information regarding porosity, modulus, strain, tensile stress and load. When compared to data from regular micropaper (Yousefi et al. 2013), it can be seen that nanopapers definitely presented improved properties in all cases, but especially nanopapers made with fibers treated with organosolv and NaOH 7.5 % where the modulus was increased to 5.3 and 5.6 GPa, respectively, whereas the modulus of micropaper is 2 GPa. As for strain, the values corresponding to organosolv and NaOH 7.5 % were 4.19 and 2.85 %, respectively; the strain of micropaper is 1.5 %.

In Fig. 8, the modulus is shown as a function of the relative density ρ/ρ_s (relationship between cellulose nanopaper density and standard density of cellulose). It can be seen how the relative density of the papers with the best mechanical properties was located between 0.75 and 0.8 with a modulus close to 5 GPa.

When focusing on the properties, at first glance, it can be observed that the nanopapers were flexible even after five to ten cycles of folding-unfolding without losing their shape due to low modulus as shown in Fig. 9b. The low modulus is often related to fiber orientation. The paper presents high opacity as can be seen in Fig. 9c, this may imply the presence of agglomerations in the inner structures. This is also a possible reason for the low modulus and stress values.

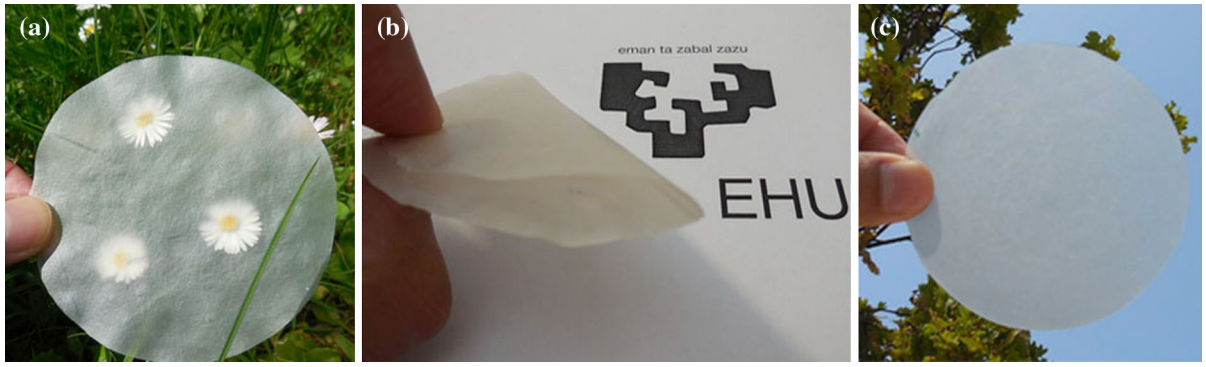

Fig. 9 Images of nanopaper obtained with the NaOH 7.5 % treatment. **a** Attempt to illustrate optical transparency when close to objects, **b** texture after 5 cycles of folding–unfolding and **c** Attempt to illustrate optical translucidity

Conclusions

Characterization performed using TAPPI standards and XRD showed high crystallinity of cellulose and therefore high crystallinity in almond shells. Chemical methods for the removal of non-cellulosic components were effective, providing pure cellulose pulps, as confirmed by FT-IR and TGA analysis. XRD also showed that hydrolysis increased the crystallinity. The AFM images demonstrated that the mechanical homogenization method was effective for obtaining nanofibers, providing fibers with a diameter ranging between 0.4 and 0.8 nm.

The nanopapers obtained in this study were flexible and translucent and exhibited improved mechanical properties compared to micropaper. The best nanopapers were those made by the organosolv and NaOH 7.5 % processes. NaOH 7.5 % represents a very effective lignin elimination process to eliminate non-cellulosic components. The nanopaper obtained by this method presented lower mechanical properties than most previous studies, since low aspect ratio and fiber orientation in the paper structure may have a direct relation to the stress distribution in the paper structure.

Acknowledgments The authors would like to thank the the Department of Education, Universities and Investigation of the Basque Government (IT672-13) for financially supporting this work. E. Robles would like to acknowledge the financial support of CONACyT, Mexico through scholarship No. 216178. The authors would like to thank Dr. Alfred D. French for the valuable advices for the preparation of the paper.

References

Alemdar A, Sain M (2008) Isolation and characterization of nanofibers from agricultural residues-wheat straw and soy hulls. Biores Technol 99:1664–1671

Annergren GE (1996) The properties of bleached pulp. Strength properties and characteristics of bleached chemical and mechanical pulps, in: pulp bleaching—principles and practice, section VII: the properties of bleached pulp. Tappi Press, Atlanta, pp 717–748

Arni AS, Zilli M, Converti A (2007) Solubilization of lignin components of food concern from sugar cane bagasse by alkaline hydrolysis. Cienc Technol Aliment 5:271–277

Bidlack J, Malone M, Benson R (1992) Molecular structure and component integration of secondary cell walls in plants. Proc Oklahoma Acad Sci 72:51–56

Buschle-Diller G, Inglesby MK, Wua Y (2005) Physicochemical properties of chemically and enzymatically modified cellulosic surfaces. Coll Surf 260:63–70

Charreau H, Foresti ML, Vázquez A (2013) Nanocellulose patents trends: a comprehensive review on patents on cellulose nanocrystals, microfibrillated and bacterial cellulose. Recent Pat Nanotechnol 7:56–80

Chen W, Yu H, Liu Y, Chen P, Zhang M, Hai Y (2011a) Individualization of cellulose nanofibers from wood using high-intensity ultrasonication combined with chemical pretreatments. Carbohydr Polym 83:1804–1811

Chen W, Yu H, Liu Y, Hai Y, Zhang M, Chen P (2011b) Isolation and characterization of cellulose nanofibers from four plant cellulose fibers using a chemical-ultrasonic process. Cellular 18:433–442

Dapía S, Santos V, Parajo JC (2002) Study of formic acid as an agent for biomass fractionation. Biomass Bioenerg 22: 213–221

Delmer C, Amor Y (1995) Cellulose biosynthesis. Plant Cell 7(7):987–1000

Escarnota E, Aguedo M, Paquot M (2011) Characterization of hemicellulosic fractions from spelt hull extracted by different methods. Carbohyd Polym 85:419–428

Fratzl P (2003) Cellulose and collagen: from fibres to tissues. Curr Opin Coll Interface Sci 8:32–39

French A (2013) Idealized powder diffraction patterns for cellulose polymorphs. Cellulose. doi:10.1007/s10570-013-0030-4

French A, Cintrón MS (2013) Cellulose polymorphy, crystallite size, and the Segal Crystallinity Index. Cellulose 20:583–588

Gibson LJ, Ashby MF (1997) Cellular solids—structure and properties, 2nd edn. Cambridge University Press, Cambridge

Henriksson M, Berglund LA, Isaksson P, Lindström T, Nishino T (2008) Cellulose nanopaper structures of high toughness. Biomacromolecules 9:1579–1585

Iwamoto S, Lee S, Endo T (2014) Relationship between aspect ratio and suspensión viscosity of wood cellulose nanofibers. Polym J 46:73–76

Jonoobi M, Harun J, Shakeri A, Misra M, Oksman K (2009) Chemical composition, crystallinity, and thermal degradation of bleached and unbleached kenaf bast pulp and nanofibers. Bioresources 4:626–639

Lee SY, Chun SJ, Kang IA, Park JY (2009) Preparation of cellulose nanofibrils by high-pressure homogenizer and cellulose-based composite films. J Ind Eng Chem 15:50–55

Li R, Fei J, Cai Y, Li Y, Feng J, Yao J (2009) Cellulose whiskers extracted from mulberry: a novel biomass production. Carbohydr Polym 76:94–99

Maiti S, Jayaramudub J, Das K, Reddy SM, Sadiku R, Ray S, Liu D (2013) Preparation and characterization of nanocellulose with new shape from different precursor. Carbohydr Polym 98:562–567

Moran J, Alvarez V, Cyras V, Vazquez A (2008) Extraction of cellulose and preparation of nanocellulose from sisal fibers. Cellular 15:149–159

Ni Y, Van Heiningen ARP (1996) Lignin removal from Alcell® pulp by washing with ethanol and water. Tappi J 79: 239–243

Pelissari F, Amaral Sobral P, Menegalli F (2014) Isolation and characterization of cellulose nanofibers from banana peels. Cellulose 21:417–432

Pirayesh H, Khazaeian A (2012) Using almond (*Prunus amygdalus* L.) shell as a bio-waste resource in wood based composite. Compos B 43:1475–1479

Rowell R (1983) The chemistry of solid wood in advances in chemistry series. American Chemical Society, Washington DC, pp 70–72

Sehaqui H, Liu A, Zhou Q, Berglund LA (2010) Fast preparation procedure for large, flat cellulose and cellulose/inorganic nanopaper structures. Biomacromolecules 11:2195–2198

Serrano L, Urruzola I, Nemeth D, Belafi-Bako K, Labidi J (2011) Modified cellulose microfibrils as benzene adsorbent. Desalination 270:143–150

Sun CC (2008) Mechanism of moisture induced variations in true density and compaction properties of microcrystalline cellulose. Int J Pharm 346:93–101

Sun RC, Tomkinson J, Wang YX, Xiao B (2000) Physicochemical and structural characterization of hemicelluloses from wheat straw by alkaline peroxide extraction. Polymer 41:2647–2656

Sun R, Sun XF, Liu GQ, Fowler P, Tomkinson J (2002) Structural and physicochemical characterization of hemicelluloses isolated by alkaline peroxide from barley straw. Polym Int 51:117–124

Sun JX, Sun XF, Zhao H, Sun RC (2004a) Isolation and characterization of cellulose 553 from sugarcane bagasse. Polym Degrad Stab 84:331–339

Sun XF, Sun RC, Fowler P, Baird MS (2004b) Isolation and characterization of cellulose obtained by a two-stage treatment with organosolv and cyanamide activated hydrogen peroxide from wheat straw. Carbohydr Polym 55:379–391

TAPPI (2007) TAPPI Standards, in TAPPI test methods, Atlanta, GA, USA

Urruzola I, de Andres MA, Nemeth D, Belafi-Bako K, Labidi J (2013a) Multicomponents adsorption of modified cellulose microfibrils. Desalin Water Treat 51:10–12

Urruzola I, Serrano L, Llano-Ponte R, Andrés MA, Labidi J (2013b) Obtaining of eucalyptus microfibrils for adsorption of aromatic compounds in aqueous solution. Chem Eng J 229:42–49

Vincent JF (1999) From cellulose to cell. J Exp Biol 202:3263–3268

Wang B, Sain K, Oksman M (2007) Study of structural morphology of hemp fiber from the micro to the nanoscale. Appl Compos Mater 14:89–103

Yousefi H, Hejazi S, Mousavi M, Azusa Y, Heidari AH (2013) Comparative study of paper and nanopaper properties prepared from bacterial cellulose nanofibers and fibers/ground cellulose nanofibers of canola straw. Ind Crop Prod 43:732–737

Yuan J, Yu Y, Wang Q, Fan X, Chen S, Wang P (2013) Modification of ramie with 1-butyl-3-methylimidazolium chloride ionic liquid. Fiber Polym 14:1254–1260

Zuluaga R, Mondragon I, Gañan P (2009) New approaches to cellulose microfibril isolation from Musaceae agro-industrial residues. Compos Interface 16:27–37